Published in final edited form as:
Dig Dis Sci. 2009 September ; 54(9): 1908–1917. doi:10.1007/s10620-008-0583-5.

Overexpression of Mcl-1 Attenuates Liver Injury and Fibrosis in the Bile Duct–Ligated Mouse

Alisan Kahraman,
Division of Gastroenterology and Hepatology, Miles and Shirley, Fiterman Center for Digestive Diseases, Mayo Clinic College of Medicine, 200 First Street SW, Rochester, MN 55905, USA

Department of Gastroenterology and Hepatology, University Clinic Essen, 45122 Essen, Germany

Justin L. Mott,
Division of Gastroenterology and Hepatology, Miles and Shirley Fiterman Center for Digestive Diseases, Mayo Clinic College of Medicine, 200 First Street SW, Rochester, MN 55905, USA

Steven F. Bronk,
Division of Gastroenterology and Hepatology, Miles and Shirley, Fiterman Center for Digestive Diseases, Mayo Clinic College of Medicine, 200 First Street SW, Rochester, MN 55905, USA

Nathan W. Werneburg,
Division of Gastroenterology and Hepatology, Miles and Shirley, Fiterman Center for Digestive Diseases, Mayo Clinic College of Medicine, 200 First Street SW, Rochester, MN 55905, USA

Fernando J. Barreyro,
Division of Gastroenterology and Hepatology, Miles and Shirley, Fiterman Center for Digestive Diseases, Mayo Clinic College of Medicine, 200 First Street SW, Rochester, MN 55905, USA

Maria E. Guicciardi,
Division of Gastroenterology and Hepatology, Miles and Shirley, Fiterman Center for Digestive Diseases, Mayo Clinic College of Medicine, 200 First Street SW, Rochester, MN 55905, USA

Yuko Akazawa,
Division of Gastroenterology and Hepatology, Miles and Shirley, Fiterman Center for Digestive Diseases, Mayo Clinic College of Medicine, 200 First Street SW, Rochester, MN 55905, USA

Karen Braley,
Department of Pharmacology and Toxicology, Dartmouth Medical School, Hanover, NH 03755-3835, USA

Ruth W. Craig, and
Department of Pharmacology and Toxicology, Dartmouth Medical School, Hanover, NH 03755-3835, USA

Gregory J. Gores
Division of Gastroenterology and Hepatology, Miles and Shirley, Fiterman Center for Digestive Diseases, Mayo Clinic College of Medicine, 200 First Street SW, Rochester, MN 55905, USA

Gregory J. Gores: gores.gregory@mayo.edu

Abstract

Correspondence to: Gregory J. Gores, gores.gregory@mayo.edu.

Hepatocyte apoptosis contributes to liver injury and fibrosis after cholestatic injury. Our aim was to ascertain if the anti-apoptotic protein Mcl-1 alters liver injury or fibrosis in the bile duct–ligated mouse. Markers of apoptosis and fibrosis were compared in wild-type and transgenic mice expressing human Mcl-1 after bile duct ligation. Compared to hMcl-1 transgenic animals, ligated wild-type mice displayed a significant increase in TUNEL-positive cells and in caspase 3/7-positive hepatocytes. Consistent with apoptotic injury, the pro-apoptotic protein Bak underwent a conformational change to an activated form upon cholestatic injury, a change mitigated by hMcl-1 overexpression. Likewise, liver histology, number of bile infarcts, serum ALT values, markers of hepatic fibrosis, and animal survival were improved in bile duct–ligated mice transgenic for hMcl-1 as compared to wild-type mice. In conclusion, increased Mcl-1 expression plays a role in hepatoprotection upon cholestatic liver injury.

Keywords

Apoptosis; Bile infarct; Liver fibrosis; Stellate cells

Introduction

Cholestasis, a pathophysiologic syndrome defined as an impairment in bile formation or flow, is characterized by retention of toxic bile acids within the liver and serum [1,2]. The increased tissue concentrations of bile acids elicit a toxic response, especially death-receptor-mediated hepatocyte apoptosis [3]. For example, numerous studies have consistently demonstrated that many toxic bile acids trigger oligomerization of the Fas death receptor in hepatocytes and cell lines culminating in a classic Fas death-receptor cascade [4–10]. The assembly of the Fas death-receptor signaling complex occurs independent of Fas ligand by a complex mechanism involving NADPH oxidase, the Src kinase termed Yes, and the epidermal growth factor receptor [6,7]. Furthermore, mice genetically deficient in Fas have reduced liver injury following BDL [4]. TRAIL also contributes to cholestatic liver injury as toxic bile acids increase expression of its cognate death receptor, DR5/TRAIL receptor-2 [11] and TRAIL-deficient mice are protected from BDL-induced injury [12]. Fas and DR5/TRAIL receptor-2 both initiate apoptosis by recruiting the zymogen pro-caspase 8 to a receptor complex where it is auto-activated by induced proximity [13]. Active caspase 8 in turn cleaves the pro-apoptotic BH3-only protein Bid generating truncated or tBid [14]. This 15-kDa protein translocates to mitochondria where it induces mitochondrial dysfunction, resulting in activation of effector caspases (e.g., caspase 3, 7, and 6) causing cellular demise. Inhibition of Bid expression by antisense technology and/or caspase activity by a protease inhibitor also attenuates cholestatic liver injury consistent with this cytotoxic signaling cascade [15,16].

Cell death in hepatocytes following death-receptor ligation is dependent upon mitochondrial outer membrane permeabilization and cytochrome *c* release [17]. This release is likely due to activation of Bax and Bak by tBid. For instance, mice deficient for both Bak and Bax survive a dose of Fas agonistic antibody that is fatal for either Bakdeficient or Bax-deficient mice [18]. Further, Bid is upstream of Bak and Bax, as Bid-deficient mice fail to manifest Bax translocation to mitochondria after Fas agonistic antibody treatment. The activation of Bax and Bak, both multidomain pro-apoptotic members of the Bcl-2 family, depend upon a conformational change that exposes the N-terminus to antibody detection [19,20], as well as oligomerization [21–23].

In hepatocytes, death-receptor signaling cascades involving tBid are blocked at the level of the mitochondria by anti-apoptotic members of the Bcl–2 family which include Bcl-2, Bcl-$X_{L,}$ Mcl-1, Bcl-w, Boo and A1 [15]. Bcl-2, richly expressed by hematopoietic cells, is not expressed by hepatocytes, although transgenic expression of Bcl-2 is protective against Fas-mediated

liver injury [24]. Bcl-w and Boo are predominantly expressed by testicular and ovarian tissue, respectively, and are not known to modulate liver cell apoptosis [25,26]. Due to difficulties in raising specific antisera, the protein expression of A1 in liver tissue has been difficult to define. Bcl-X_L is constitutively expressed by hepatocytes and conditional hepatic deletion of this gene in mice results in spontaneous hepatocyte apoptosis [27], while overexpression of Bcl-X_L provides a survival advantage to hepatocytes [28]. Although Mcl-1 is expressed in wild-type hepatocytes, the level of expression is not sufficient to prevent Fas- nor Concanavalin A-mediated hepatocyte apoptosis [29]. However, whether Mcl-1 overexpression is sufficient to ameliorate liver injury in a disease model such as cholestasis remains unclear.

Therefore, the overall objective of this study was to determine if mice transgenic for human Mcl-1 (hMcl-1 Tg) are resistant to obstructive cholestatic liver injury following bile duct ligation (BDL). To address our objective we formulated the following two questions: (i) during cholestasis, is hepatocyte apoptosis reduced by transgenic expression of hMcl-1; and (ii) are liver injury, hepatic fibrosis, and overall animal survival improved by overexpression of hMcl-1. The results of this study support a critical role for Mcl-1 in modulating murine cholestatic liver injury following obstructive cholestasis by BDL.

Materials and Methods

Animal Models

The care and use of the animals for these studies were reviewed and approved by the Institutional Animal Care and Use Committee (IACUC) at Mayo Clinic. Mice were maintained in a temperature-controlled (22°C), pathogenfree environment and fed a standard rodent chow diet and water ad libitum. C57/BL6 wild-type and human Mcl-1 transgenic (hMcl-1 Tg) mice (6–8 weeks-of-age, 20–25 g body weight) were employed for these studies. The hMcl-1 Tg mice were generated previously [30]. Briefly, a minigene including all Mcl-1 exons and introns, as well as approximately 10.5 kb of 5′ genomic flanking sequence (including presumptive regulatory sequences) and 1.7 kb of 3′ flanking sequence was used to generate founder transgenic mice on a C57B6/SJL-F1 background. These were then mated with C57/BL6 mice and have been maintained as homozygous transgenic mice on the C57/ BL6 background. Mice expressing the human Mcl-1 transgene do not exhibit phenotypic changes in the liver. However, they do show a moderate splenic enlargement, which is associated with increased numbers of B and T lymphocytes and also exhibit an expansion of the myeloid relative to the lymphoid compartment in the bone marrow.

For experimental procedures, mice were anesthetized with ketamine 60 mg/kg plus xylazine 10 mg/kg body weight by intraperitoneal injection. After a midline upper-abdominal incision, the peritoneal cavity was opened, the abdominal wall retracted, and the common hepatic bile duct was double-ligated and divided between the ligatures as previously described by us in detail [4]. Sham-operated wild-type mice, used as controls, underwent laparotomy with exposure but without ligation of the common bile duct. The fascia and skin were closed with sterile surgical 5–0 sutures (ETHICON Inc., Somerville, NJ). About 7 or 14 days after BDL, depending on the experimental procedures, mice were re-anesthetized and blood was obtained from the inferior vena cava for serum ALT and total bilirubin determinations prior to procuring liver tissue for additional studies (vide infra) [31]. The liver was removed and cut into small pieces and either snap-frozen in liquid nitrogen for storage at −80°C or fixed in freshly prepared 4% paraformaldehyde in phosphate-buffered saline (PBS) for 24 h at 4°C. Liver sections were also subjected to RNA extraction using the Trizol reagent (Invitrogen, Carlsbad, CA).

Histopathology

For histological review of hematoxylin and eosin (H&E)-stained liver sections by light microscopy (Nikon Eclipse Meta Morph V 5.0.7, West Lafayette, IN), the liver was diced into 5×5 mm^2 sections, fixed in 4% paraformaldehyde for 48 h, and then embedded in paraffin (Curtin Matheson Scientific Inc., Houston, TX). Tissue sections (4 μm) were prepared using a microtome (Reichert Scientific Instruments, Buffalo, NY) and placed on glass slides. H&E staining was performed according to standard techniques.

TUNEL Assay and Immunofluorescence

Apoptotic cells were quantitated by the terminal deoxynucleotidyl transferase-mediated dUTP nick-end labeling (TUNEL) assay which enzymatically labels free 3′-OH ends of damaged DNA with a fluorescently labeled nucleotide as we have previously described in detail [32]. TUNEL-labeled cells (i.e., fluorescent nuclei) were quantified by counting the number of positive cells per high-power field. A total of ten high-power fields were analyzed for each animal with excitation and emission wavelengths of 488 and 507 nm, respectively, using an inverted laser scanning confocal microscope (LSM 510, Carl Zeiss Micro-Imaging Inc., Thornwood, NJ) equipped with a 40× NA 1.4 lens and LSM 510 imaging software. Data were expressed as the number of TUNEL-positive cells/10 high-power field (hpf).

Immunofluorescence analysis for activated caspases 3/7 was performed using a rabbit anti-active caspase 3/7 polyclonal antibody (BD Biosciences/Pharmingen, San Diego, CA) recognizing a common neo-epitope shared by activated caspases 3 and 7 as we have previously described [32]. Immunofluorescence staining for the N-terminus of Bak, exposed upon Bak activation, was performed using a rabbit polyclonal antibody (Bak-NT, Upstate, Lake Placid, NY). The liver specimens were viewed by confocal microscopy using excitation and emission wavelengths of 577 and 590 nm, respectively, for activated Caspase 3/7 and 488 and 507, respectively, for activated Bak. The number of caspase 3/7-positive or Bak-NT-positive cells was quantified per 10 high-power fields as described above for the TUNEL assay.

Quantitative Reverse-Transcription Polymerase Chain Reaction (RT-PCR)

Total RNA was isolated from liver tissue using the Trizol reagent (Invitrogen, Carlsbad, CA). For each RNA sample, a 10-μg aliquot was reverse-transcribed into complementary DNA using a random primer and Maloney murine leukemia virus (MMLV) reverse transcriptase (Invitrogen) as previously described in detail [33]. The cDNA template was then PCR amplified with Taq DNA polymerase (Invitrogen) using standard protocols. Quantitation of α-SMA and collagen 1α (I) were performed using a Light Cycler (Roche Diagnostics Corp., Mannheim, Germany) and SYBR green as the fluorophore (Invitrogen); the detailed procedure and primer sequences have been recently described [12].

Immunoblot Analysis

Liver tissue was directly lysed for 30 min on ice with lysis buffer consisting of 50 mM Tris–HCl (pH 7.4), 1% Nonidet P-40, 0.25% sodium deoxycholate, 150 mM NaCl, 1 mM EDTA, 1 mM PMSF, 1 μg/ml aprotinin, 1 μg/ml leupeptin, 1 μg/ml pepstatin, 10 mM Na_3VO_4, and 1 mM NaF. After centrifugation at 13,000 × *g* for 15 min at 4°C, protein concentration in the supernatant was measured using Bradford reagent (Bio-Rad, Hercules, CA). Protein was denatured by boiling for 10 min in Laemmli sample buffer (Bio-Rad). Protein (50 ug) was resolved by SDS-PAGE on a gradient gel and then transferred onto nitrocellulose membranes. Blocking was carried out using 5% non-fat dairy milk in Tris-buffered saline (20 mM Tris, 150 mM NaCl, pH 7.4) with 0.1% Tween-20 for 1 h at room temperature. Primary antibodies were diluted 1:1,000 in blocking solution and incubated overnight at 4°C. The following antibodies were used: total Bak (Calbiochem, San Diego, CA), Bim (Chemicon, Australia),

Bax, Bcl-X_L, Bid, Fas (all from Santa Cruz Biotechnology Inc., Santa Cruz, CA), c-FLIP (Upstate Biotechnology, Lake Placid, NY), hMcl-1 (BD Biosciences/Pharmingen, San Diego, CA), and γ-Tubulin (Sigma-Aldrich Corp., St. Louis, MO). Membranes were incubated (45 min at room temperature) in horseradish-peroxidase conjugated secondary antibodies (Biosource International, Camarillo, CA) diluted 1:3,000 in blocking solution. Immune complexes were visualized using chemiluminescent substrate (ECL, Amersham, IL) and Kodak X-OMAT film (Eastman Kodak, Rochester, NY) according to the manufacturer's instructions.

Immunohistochemistry for α-Smooth Muscle Actin (α-SMA) and Determination of Liver Fibrosis by Sirius Red Staining

The sections were stained for α-SMA using a mouse monoclonal antibody (NeoMarkers, Fremont, CA), which is pre-diluted in 50 mM Tris–HCl, pH 7.6, containing stabilizing protein and 15 mM sodium azide by the manufacturer for staining formalin-fixed, paraffin-embedded tissues. The sections were incubated with the primary antibody overnight at 4°C in a dilution 1:200. Negative control slides were incubated with non-immune immunoglobulin under the same conditions. Secondary reagents were obtained from the Dako Cytomation EnVision + System-HRP ready-to-use kit (Dako Cytomation Inc., Carpinteria, CA); 3,3′-diaminobenzidine (DAB) chromogen solution was used for visualization by light microscopy. Finally, the tissue was counterstained with hematoxylin for 3 min. Liver fibrosis was quantified using Sirius red staining as described by Arteel and colleagues [34]. Direct red 80 and Fast-green FCF were obtained from Sigma-Aldrich Diagnostics. Liver sections were stained and red-stained collagen fibers were quantified by digital image analysis as previously described by us in detail [31].

Statistical Analysis

All data represent at least five separate experiments and are expressed as the mean ± standard error unless otherwise indicated. Differences between groups were compared using analysis of variance (ANOVA) for repeated measures and post-hoc Bonferroni test to correct for multiple comparisons. A *P*-value less than 0.05 was considered to be statistically significant. All statistical analyses were performed using In-Stat Software (Graph Pad, San Diego, CA).

Results

Hepatocyte Apoptosis is Significantly Reduced in the BDL hMcl-1 Tg Mouse

Before embarking on a series of studies assessing apoptosis and liver injury, we provided assurance that expression of apoptosis modulating proteins was similar between both genotypes. Immunoblot analysis was performed for several apoptosis effector proteins including Fas, Bax, Bak, Bim, c-FLIP, Bid, Bcl-X_L and hMcl-1 (Fig. 1). Hepatic protein levels for these key apoptotic effectors were similar other than the expected observation of hMcl-1 in the hMcl-1 Tg mouse. A cross-reacting band was consistently observed migrating slightly faster than hMcl-1 in extracts from wild-type mice. Next, to examine the effects of Mcl-1 in mediating hepatic apoptosis, wild-type and hMcl-1 Tg mice were subjected to BDL for 7 days. Liver specimens from wild-type animals demonstrated numerous clusters of apoptotic cells in a background of altered hepatic microarchitecture (Figs. 2a, 3a). Quantitation of these TUNEL-positive cells demonstrated frequent apoptotic cells in wild-type BDL mice as compared to sham-operated wild-type and hMcl-1 Tg controls. By contrast, TUNEL-positive cells were significantly reduced in BDL hMcl-1 Tg animals compared to wild-type BDL mice (Fig. 2a).

The activation of executioner caspases, especially caspases 3 and 7 (which share a neo-epitope upon cleavage), is a biochemical hallmark of apoptosis [35]. Therefore, to further confirm that hepatocyte apoptosis occurs in wild-type animals following BDL, we next performed

immunohistochemistry for activated caspase 3/7. Immunoreactive product was readily identified in liver tissues from wild-type mice following BDL, but not in sham-operated wild-type (Fig. 2b) and hMcl-1 Tg controls (not shown). Consistent with results from the TUNEL assay, BDL wild-type animals demonstrated numerous caspase 3/7-positive hepatocytes versus sham-operated controls (Fig. 2b). Caspase 3/7-positive cells were also significantly reduced in BDL hMcl-1 Tg mice as compared to wild-type animals. Taken together, these data demonstrate that overexpression of hMcl-1 is cytoprotective and attenuates hepatocyte apoptosis in BDL mice.

The pro-apoptotic transmembrane protein Bak participates in apoptosis by promoting mitochondrial permeabilization and release of cytochrome c upon a death-inducing stimulus [23]. Indeed, Mcl-1 is thought to counteract the effects of pro-apoptotic Bcl-2 family proteins by its action at the mitochondrial membrane to prevent permeabilization [36]. Thus, we investigated the activation of Bak after BDL injury by immunofluorescence for the N-terminal domain of Bak. Under basal conditions (i.e., sham-operated wild-type), the Bak N-terminus is not accessible to antibody interaction due to its location within the protein. However, upon activation, Bak undergoes a conformational change that exposes the N-terminus to antibody interaction. We observed that experimental cholestasis was associated with increased Bak N-terminal immunoreactivity in wild-type mice which was significantly reduced in hMcl-1 Tg mice following BDL (Fig. 2c). These observations are consistent with Bak activation in obstructive cholestasis by a Mcl-1 regulated process.

Liver Injury is Significantly Reduced in hMcl-1 Tg Mice Following BDL

To further examine the ability of Mcl-1 to attenuate liver injury following BDL, histopathological examination of liver specimens was performed along with determinations of serum ALT values. Histopathology from 7-day BDL wild-type mice displayed severe cholestatic hepatitis with widespread bile infarcts—a pathognomonic feature of large bile duct obstruction—along with bile ductular proliferation, portal edema, and hepatocellular damage. The cholestatic hepatitis of liver injury was again markedly reduced in specimens from hMcl-1 Tg animals following 7 days of BDL. These animals displayed almost intact liver morphology (Fig. 3a). In addition, bile infarcts were less evident in BDL hMcl-1 Tg mice (Fig. 3b). A significant reduction in serum ALT values in hMcl-1 Tg animals was also observed 7 days following BDL as compared to wild-type mice (Fig. 3c). Differences in liver injury could not be ascribed to differences in experimental cholestasis because total bilirubin levels in BDL mice were almost identical indicating similar cholestatic effects of the BDL between both mouse strains (Fig. 3d, P = NS). Thus, these data suggest that overexpression of hMcl-1 protein is hepatoprotective during murine obstructive cholestasis.

Markers of Hepatic Fibrogenesis Are Attenuated in hMcl-1 Tg Animals Following BDL for 14 days

If the reduction of liver injury in hMcl-1 Tg mice is significant, it should also translate into reduced hepatic fibrosis—a sequela of liver damage. Because hepatic myofibroblasts are the principal cell type responsible for collagen deposition in the liver [37,38], we next quantified transcripts indicative of myofibroblast activation by quantitative real time-PCR. After 14 days of BDL, mRNA for α-smooth muscle actin, a cardinal marker for stellate cell activation, was increased 11-fold in wild-type as compared to sham-operated wild-type and hMcl-1 Tg mice. More importantly, the transcript for α-SMA was significantly reduced in BDL hMcl-1 Tg animals (Fig. 4a). Consistent with the mRNA data, α-SMA immunoreactivity was also increased in the sinusoids of BDL wild-type mice but markedly reduced in BDL hMcl-1 Tg mice (Fig. 4b). To ascertain if stellate cell activation was also associated with enhanced hepatic fibrogenesis, mRNA for hepatic collagen 1α (I) was quantified. Indeed, collagen 1α (I) mRNA expression was increased 12-fold in BDL wild-type versus sham-operated wild-type or hMcl-1

Tg mice, while hMcl-1 Tg animals showed a more modest (5-fold) increase in collagen 1α (I) mRNA following BDL for 14 days (Fig. 4c). Hepatic collagen protein deposition was further identified in liver specimens by Sirius red staining (Fig. 4d) and subjected to quantitative morphometry as previously described by us in detail [31]. Collagen staining by Sirius red was also significantly reduced in BDL hMcl-1 Tg versus BDL wild-type mice (Fig. 4d). Collectively, these data suggest that following bile duct ligation for 14 days, stellate cell activation and hepatic fibrogenesis are attenuated in BDL hMcl-1 Tg mice, likely secondary to the reduced liver injury observed in this mouse strain.

Survival of hMcl-1 Tg Animals Is Enhanced Following BDL

Given that liver injury and fibrosis are significantly reduced in BDL hMcl-1 Tg mice, we reasoned that animal survival may be enhanced. Animal survival is likely influenced by the magnitude of the initial insult, including hepatocyte apoptosis, as well as the fibrotic response, in addition to more generalized physiologic insult resulting from the complete ligation of the common bile duct. Therefore, in our final study, we examined overall animal survival after BDL. By day 14 after BDL, 80% of the hMcl-1 Tg animals were still alive compared to only 20% in the wild-type animal group (Fig. 5). The observation that maximal cholestatic liver injury is followed by impaired survival is consistent with prior experience in this model and suggests that death is multifactorial and liver injury only one component of the lethal insult. However, as hMcl-1 expression reduces apoptotic liver injury and fibrosis, hepatoprotection likely, in part, contributes to the improved animal survival. Taken together, this study clearly demonstrates that during cholestasis, overexpression of hMcl-1 exerts an important pro-survival effect. Given that hMcl-1 expression is not liver-specific, the organ-specific effects responsible for enhanced animal survival can not be specifically delineated.

Discussion

The results of this study pertain to the ability of Mcl-1 to modulate cholestatic liver injury in obstructive murine cholestasis following BDL. Following BDL of wild-type mice, there is extensive liver injury, as determined by serum transaminase levels, Bak activation, caspase-3/7 activation, and hepatocyte apoptosis. The data demonstrate that transgenic expression of the human Mcl-1 protein is sufficient to attenuate these markers of hepatocyte apoptosis and liver injury, as well as subsequent hepatic fibrosis in this model. These data further provide a link between hepatocyte apoptosis and liver injury during cholestasis. In addition, the data suggest that enhanced Mcl-1 expression may be salutary in cholestatic liver diseases and provide new information regarding the pro-survival effects of Mcl-1 during obstructive cholestasis. Each of these findings will be discussed in below in greater detail.

In the current study, we demonstrated that mice transgenic for hMcl-1 exhibited reduced hepatocyte apoptosis and liver injury following 7 days of BDL. Hepatocyte growth factor and constitutive androstane receptor-stimulated Mcl-1 expression have been shown to block acute Fas-mediated liver injury [29,39]. Moreover, Mcl-1 binding and sequestering of truncated Bid in death-receptor mediated-apoptosis has also been reported [15]. Our present data extend these observations by demonstrating hMcl-1 cytoprotection during a subacute disease model of death-receptor-mediated liver injury, obstructive cholestasis. Activation of the mitochondrial apoptotic program is necessary for death-receptor mediated cell death of type II cells, such as hepatocytes [40]. The mechanism of protection afforded by Mcl-1 is likely due to inhibition of mitochondrial Bak activation. Cytoprotection by the antiapoptotic protein hMcl-1 is consistent with a predominant role for apoptosis in liver injury during obstructive cholestasis, and is consistent with apoptosis by death receptors.

Hepatic fibrosis is mediated by activation of HSC which transdifferentiate into myofibroblasts and secrete collagen type I and III, which are the collagens responsible for liver fibrosis.

Additionally, portal mesenchymal cells likely contribute significantly to fibrosis [38]. Fibrosis is increasingly recognized as a dynamic process, where hepatocyte injury and death induce activation of HSC causing fibrosis which is reversible upon apoptotic removal of myofibroblasts. Indeed, induction of HSC apoptosis by gliotoxin or sulfasalazine reduces hepatic fibrosis, while myofibroblast overexpression of the antiapoptotic protein Bcl-2 promotes hepatic fibrogenesis [41,42]. Thus, transgenic expression of hMcl-1 could have opposing effects on fibrosis; potentially promoting fibrosis by maintaining the viability of activated myofibroblasts, or on the contrary, hMcl-1 expression may protect from fibrosis by mitigating the fibrogenic stimulus, hepatocyte injury, and apoptosis. The reduced hepatic fibrosis is best explained by the observed reduction in hepatocyte apoptosis in hMcl-1 mice.

Hepatocyte apoptosis can activate myofibroblasts by two potential mechanisms. The cellular remnants of apoptotic hepatocytes can be phagocytosed by either Kupffer and/or stellate cells [43,44]. This phagocytic process activates both cell types. Kupffer cell engulfment of apoptotic bodies results in expression of TGF-β, a profibrogenic cytokine that activates stellate cells by a paracrine mechanism [45]. Alternatively, phagocytosis of apoptotic bodies directly by stellate cells also results in their expression of TGF-β which, in a cell autonomous manner, may drive activation by an autocrine process [44]. Either cellular mechanism could account for the reduction of hepatic fibrosis afforded by inhibition of hepatocyte apoptosis in the current study. Taken together, the current data provide further evidence of a mechanistic link between hepatocyte apoptosis and liver fibrosis.

Compared to other anti-apoptotic Bcl-2 family proteins, Mcl-1 is unique because of rapid and robust regulation of its mRNA and protein expression. Mcl-1 is rapidly inducible by transcription factors such as STAT3 and NF-κB, translation is regulated by miRNA and ERK 1/2 signaling pathways, and post-translationally it is regulated by phosphorylation and ubiquitinylation [46–52]. These multiple levels of regulation render cellular Mcl-1 protein levels susceptible to pharmacologic manipulation. For example, a constitutive androstane receptor agonist, proteasome inhibitors, and glycogen synthase kinase-3 inhibitors increase cellular protein levels of Mcl-1 [29,51]. In this regard, it may be possible to increase hepatic Mcl-1 levels to minimize liver injury and fibrosis in cholestatic syndromes. This hepatoprotective strategy merits further examination.

Abbreviations

ALT	Alanine aminotransferase
AST	Aspartate aminotransferase
α-SMA	α-Smooth muscle actin
BDL	Bile duct ligation/–ligated
hMcl-1	Human myeloid cell leukemia-1
HSC	Hepatic stellate cell
Tg	Transgenic
TUNEL	Terminal deoxynucleotidyl transferase-mediated dUTP nick-end labeling
wt	Wild-type

Acknowledgments

This work was supported by a fellowship grant from the Association for Scientific Research and Science at the Department of Gastroenterology and Hepatology, University Clinic Essen, Duisburg-Essen University, 45122—Germany to A. K. and by Grant DK 41876 from the National Institute of Health to G. J. G., as well as the Mayo

Foundation Rochester, Minnesota, USA. The authors thank Erin Nystuen-Bungum for her excellent secretarial assistance and James Tarara from the Division of Biochemistry and Molecular Biology (Mayo Clinic, Rochester, MN) for quantitation of the Sirius red images.

References

1. Miyai K, Richardson AL, Mayr W, Javitt NB. Subcellular pathology of rat liver in cholestasis and choleresis induced by bile salts. 1. Effects of lithocholic, 3beta-hydroxy-5-cholenoic, cholic and dehydrocholic acids. Lab Invest 1977;36:249–258. [PubMed: 839737]
2. Schmucker DL, Ohta M, Kanai S, Sato Y, Kitani K. Hepatic injury induced by bile salts: correlation between biochemical and morphological events. Hepatology 1990;12:1216–1221. doi:10.1002/hep.1840120523. [PubMed: 2227821]
3. Guicciardi ME, Gores GJ. Bile acid-mediated hepatocyte apoptosis and cholestatic liver disease. Dig Liver Dis 2002;34:387–392. doi:10.1016/S1590-8658(02)80033-0. [PubMed: 12132783]
4. Miyoshi H, Rust C, Roberts PJ, Burgart LJ, Gores GJ. Hepatocyte apoptosis after bile duct ligation in the mouse involves Fas. Gastroenterology 1999;117:669–677. doi:10.1016/S0016-5085(99)70461-0. [PubMed: 10464144]
5. Qiao L, Studer E, Leach K, et al. Deoxycholic acid (DCA) causes ligand-independent activation of epidermal growth factor receptor (EGFR) and FAS receptor in primary hepatocytes: inhibition of EGFR/mitogen-activated protein kinase-signaling module enhances DCA-induced apoptosis. Mol Biol Cell 2001;12:2629–2645. [PubMed: 11553704]
6. Reinehr R, Graf D, Haussinger D. Bile salt-induced hepatocyte apoptosis involves epidermal growth factor receptor-dependent CD95 tyrosine phosphorylation. Gastroenterology 2003;125:839–853. doi:10.1016/S0016-5085(03)01055-2. [PubMed: 12949729]
7. Reinehr R, Haussinger D. Inhibition of bile salt-induced apoptosis by cyclic AMP involves serine/threonine phosphorylation of CD95. Gastroenterology 2004;126:249–262. doi:10.1053/j.gastro.2003.09.044. [PubMed: 14699504]
8. Faubion WA, Guicciardi ME, Miyoshi H, et al. Toxic bile salts induce rodent hepatocyte apoptosis via direct activation of Fas. J Clin Invest 1999;103:137–145. doi:10.1172/JCI4765. [PubMed: 9884343]
9. Sodeman T, Bronk SF, Roberts PJ, Miyoshi H, Gores GJ. Bile salts mediate hepatocyte apoptosis by increasing cell surface trafficking of Fas. Am J Physiol Gastrointest Liver Physiol 2000;278:G992–G999. [PubMed: 10859230]
10. Gupta S, Natarajan R, Payne SG, et al. Deoxycholic acid activates the c-Jun N-terminal kinase pathway via FAS receptor activation in primary hepatocytes. Role of acidic sphingomyelinase-mediated ceramide generation in FAS receptor activation. J Biol Chem 2004;279:5821–5828. doi:10.1074/jbc.M310979200. [PubMed: 14660582]
11. Higuchi H, Bronk SF, Takikawa Y, et al. The bile acid glycochenodeoxycholate induces trail-receptor 2/DR5 expression and apoptosis. J Biol Chem 2001;276:38610–38618. doi:10.1074/jbc.M105300200. [PubMed: 11507096]
12. Kahraman A, Barreyro FJ, Bronk SF, et al. TRAIL mediates liver injury by the innate immune system in the bile duct–ligated mouse. Hepatology 2008;47:1317–1330. doi:10.1002/hep.22136. [PubMed: 18220275]
13. Muzio M, Stockwell BR, Stennicke HR, Salvesen GS, Dixit VM. An induced proximity model for caspase-8 activation. J Biol Chem 1998;273:2926–2930. doi:10.1074/jbc.273.5.2926. [PubMed: 9446604]
14. Luo X, Budihardjo I, Zou H, Slaughter C, Wang X. Bid, a Bcl2 interacting protein, mediates cytochrome c release from mitochondria in response to activation of cell surface death receptors. Cell 1998;94:481–490. doi:10.1016/S0092-8674(00)81589-5. [PubMed: 9727491]
15. Higuchi H, Miyoshi H, Bronk SF, Zhang H, Dean N, Gores GJ. Bid antisense attenuates bile acid-induced apoptosis and chole-static liver injury. J Pharmacol Exp Ther 2001;299:866–873. [PubMed: 11714870]
16. Canbay A, Feldstein A, Baskin-Bey E, Bronk SF, Gores GJ. The caspase inhibitor IDN-6556 attenuates hepatic injury, fibrosis in the bile duct ligated mouse. J Pharmacol Exp Ther 2004;308:1191–1196. doi:10.1124/jpet.103.060129. [PubMed: 14617689]

17. Higuchi H, Gores GJ. Bile acid regulation of hepatic physiology: IV. Bile acids death receptors. Am J Physiol Gastrointest Liver Physiol 2003;284:G734–G738. [PubMed: 12684208]

18. Wei MC, Zong WX, Cheng EH, et al. Proapoptotic BAX and BAK: a requisite gateway to mitochondrial dysfunction and death. Science 2001;292:727–730. doi:10.1126/science.1059108. [PubMed: 11326099]

19. Nechushtan A, Smith CL, Hsu YT, Youle RJ. Conformation of the Bax C-terminus regulates subcellular location and cell death. EMBO J 1999;18:2330–2341. doi:10.1093/emboj/18.9.2330. [PubMed: 10228148]

20. Griffiths GJ, Dubrez L, Morgan CP, et al. Cell damage-induced conformational changes of the pro-apoptotic protein Bak in vivo precede the onset of apoptosis. J Cell Biol 1999;144:903–914. doi: 10.1083/jcb.144.5.903. [PubMed: 10085290]

21. Antonsson B, Montessuit S, Lauper S, Eskes R, Martinou JC. Bax oligomerization is required for channel-forming activity in liposomes and to trigger cytochrome c release from mitochondria. Biochem J 2000;345(Pt 2):271–278. doi:10.1042/0264-6021:345 0271. [PubMed: 10620504]

22. Korsmeyer SJ, Wei MC, Saito M, Weiler S, Oh KJ, Schlesinger PH. Pro-apoptotic cascade activates BID, which oligomerizes BAK or BAX into pores that result in the release of cytochrome c. Cell Death Differ 2000;7:1166–1173. doi:10.1038/sj.cdd.4400783. [PubMed: 11175253]

23. Wei MC, Lindsten T, Mootha VK, et al. tBID, a membranetargeted death ligand, oligomerizes BAK to release cytochrome c. Genes Dev 2000;14:2060–2071. [PubMed: 10950869]

24. Rodriguez I, Matsuura K, Khatib K, Reed JC, Nagata S, Vassalli P. A Bcl-2 transgene expressed in hepatocytes protects mice from fulminant liver destruction but not from rapid death induced by anti-Fas antibody injection. J Exp Med 1996;183:1031–1036. doi:10.1084/jem.183.3.1031. [PubMed: 8642244]

25. Print CG, Loveland KL, Gibson L, et al. Apoptosis regulator Bclw is essential for spermatogenesis but appears otherwise redundant. Proc Natl Acad Sci USA 1998;95:12424–12431. doi:10.1073/pnas.95.21.12424. [PubMed: 9770502]

26. Song Q, Kuang Y, Dixit VM, Vincenz C. Boo, a novel negative regulator of cell death, interacts with Apaf-1. EMBO J 1999;18:167–178. doi:10.1093/emboj/18.1.167. [PubMed: 9878060]

27. Takehara T, Tatsumi T, Suzuki T, et al. Hepatocyte-specific disruption of Bcl-xL leads to continuous hepatocyte apoptosis and liver fibrotic responses. Gastroenterology 2004;127:1189–1197. doi: 10.1053/j.gastro.2004.07.019. [PubMed: 15480996]

28. Mitchell C, Mallet VO, Guidotti JE, Goulenok C, Kahn A, Gilgenkrantz H. Liver repopulation by Bcl-x(L) transgenic hepatocytes. Am J Pathol 2002;160:31–35. [PubMed: 11786395]

29. Baskin-Bey ES, Huang W, Ishimura N, et al. Constitutive androstane receptor (CAR) ligand, TCPOBOP, attenuates Fas-induced murine liver injury by altering Bcl-2 proteins. Hepatology 2006;44:252–262. doi:10.1002/hep.21236. [PubMed: 16799968]

30. Zhou P, Qian L, Bieszczad CK, et al. Mcl-1 in transgenic mice promotes survival in a spectrum of hematopoietic cell types and immortalization in the myeloid lineage. Blood 1998;92:3226–3239. [PubMed: 9787159]

31. Canbay A, Higuchi H, Bronk SF, Taniai M, Sebo TJ, Gores GJ. Fas enhances fibrogenesis in the bile duct ligated mouse: a link between apoptosis and fibrosis. Gastroenterology 2002;123:1323–1330. doi:10.1053/gast.2002.35953. [PubMed: 12360492]

32. Natori S, Selzner M, Valentino KL, et al. Apoptosis of sinusoidal endothelial cells occurs during liver preservation injury by a caspase-dependent mechanism. Transplantation 1999;68:89–96. doi: 10.1097/00007890-199907150-00018. [PubMed: 10428274]

33. Kurosawa H, Que FG, Roberts LR, Fesmier PJ, Gores GJ. Hepatocytes in the bile duct–ligated rat express Bcl-2. Am J Physiol 1997;272:G1587–G1593. [PubMed: 9227497]

34. Arteel GE, Raleigh JA, Bradford BU, Thurman RG. Acute alcohol produces hypoxia directly in rat liver tissue in vivo: role of Kupffer cells. Am J Physiol 1996;271:G494–G500. [PubMed: 8843775]

35. Cohen GM. Caspases: the executioners of apoptosis. Biochem J 1997;326(Pt 1):1–16. [PubMed: 9337844]

36. Nijhawan D, Fang M, Traer E, et al. Elimination of Mcl-1 is required for the initiation of apoptosis following ultraviolet irradiation. Genes Dev 2003;17:1475–1486. doi:10.1101/gad.1093903. [PubMed: 12783855]

37. Reeves HL, Friedman SL. Activation of hepatic stellate cells—a key issue in liver fibrosis. Front Biosci 2002;7:d808–d826. doi:10.2741/reeves. [PubMed: 11897564]
38. Beaussier M, Wendum D, Schiffer E, et al. Prominent contribution of portal mesenchymal cells to liver fibrosis in ischemic and obstructive cholestatic injuries. Lab Invest 2007;87:292–303. doi: 10.1038/labinvest.3700513. [PubMed: 17260005]
39. Schulze-Bergkamen H, Brenner D, Krueger A, et al. Hepatocyte growth factor induces Mcl-1 in primary human hepatocytes and inhibits CD95-mediated apoptosis via Akt. Hepatology 2004;39:645–654. doi:10.1002/hep.20138. [PubMed: 14999683]
40. Yin XM, Wang K, Gross A, et al. Bid-deficient mice are resistant to Fas-induced hepatocellular apoptosis. Nature 1999;400:886–891. doi:10.1038/23730. [PubMed: 10476969]
41. Novo E, Marra F, Zamara E, et al. Overexpression of Bcl-2 by activated human hepatic stellate cells: resistance to apoptosis as a mechanism of progressive hepatic fibrogenesis in humans. Gut 2006;55:1174–1182. doi:10.1136/gut.2005.082701. [PubMed: 16423888]
42. Elsharkawy AM, Oakley F, Mann DA. The role and regulation of hepatic stellate cell apoptosis in reversal of liver fibrosis. Apoptosis 2005;10:927–939. doi:10.1007/s10495-005-1055-4. [PubMed: 16151628]
43. Canbay A, Feldstein AE, Higuchi H, et al. Kupffer cell engulfment of apoptotic bodies stimulates death ligand and cytokine expression. Hepatology 2003;38:1188–1198. doi:10.1053/jhep. 2003.50472. [PubMed: 14578857]
44. Canbay A, Taimr P, Torok N, Higuchi H, Friedman S, Gores GJ. Apoptotic body engulfment by a human stellate cell line is profibrogenic. Lab Invest 2003;83:655–663. [PubMed: 12746475]
45. Roth S, Michel K, Gressner AM. (Latent) transforming growth factor beta in liver parenchymal cells, its injury-dependent release, and paracrine effects on rat hepatic stellate cells. Hepatology 1998;27:1003–1012. doi:10.1002/hep.510270416. [PubMed: 9537440]
46. Puthier D, Bataille R, Amiot M. IL-6 up-regulates mcl-1 in human myeloma cells through JAK/STAT rather than ras/ MAP kinase pathway. Eur J Immunol 1999;29:3945–3950. doi:10.1002/(SICI) 1521-4141(199912)29:12<3945::AID-IMMU 3945>3.0.CO;2-O. [PubMed: 10602002]
47. Ricci MS, Kim SH, Ogi K, et al. Reduction of TRAIL-induced Mcl-1 and cIAP2 by c-Myc or sorafenib sensitizes resistant human cancer cells to TRAIL-induced death. Cancer Cell 2007;12:66–80. doi: 10.1016/j.ccr.2007.05.006. [PubMed: 17613437]
48. Mott JL, Kobayashi S, Bronk SF, Gores GJ. mir-29 regulates Mcl-1 protein expression and apoptosis. Oncogene 2007;26:6133–6140. doi:10.1038/sj.onc.1210436. [PubMed: 17404574]
49. Boucher MJ, Morisset J, Vachon PH, Reed JC, Laine J, Rivard N. MEK/ERK signaling pathway regulates the expression of Bcl-2, Bcl-X(L), and Mcl-1 and promotes survival of human pancreatic cancer cells. J Cell Biochem 2000;79:355–369. doi:10.1002/ 1097-4644(20001201)79:3<355::AID-JCB20>3.0.CO;2-0. [PubMed: 10972974]
50. Kobayashi S, Lee SH, Meng XW, et al. Serine 64 phosphorylation enhances the antiapoptotic function of Mcl-1. J Biol Chem 2007;282:18407–18417. doi:10.1074/jbc.M610010200. [PubMed: 17463001]
51. Maurer U, Charvet C, Wagman AS, Dejardin E, Green DR. Glycogen synthase kinase-3 regulates mitochondrial outer membrane permeabilization and apoptosis by destabilization of MCL-1. Mol Cell 2006;21:749–760. doi:10.1016/j.molcel.2006.02.009. [PubMed: 16543145]
52. Zhong Q, Gao W, Du F, Wang X. Mule/ARF-BP1, a BH3-only E3 ubiquitin ligase, catalyzes the polyubiquitination of Mcl-1 and regulates apoptosis. Cell 2005;121:1085–1095. doi:10.1016/j.cell. 2005.06.009. [PubMed: 15989957]

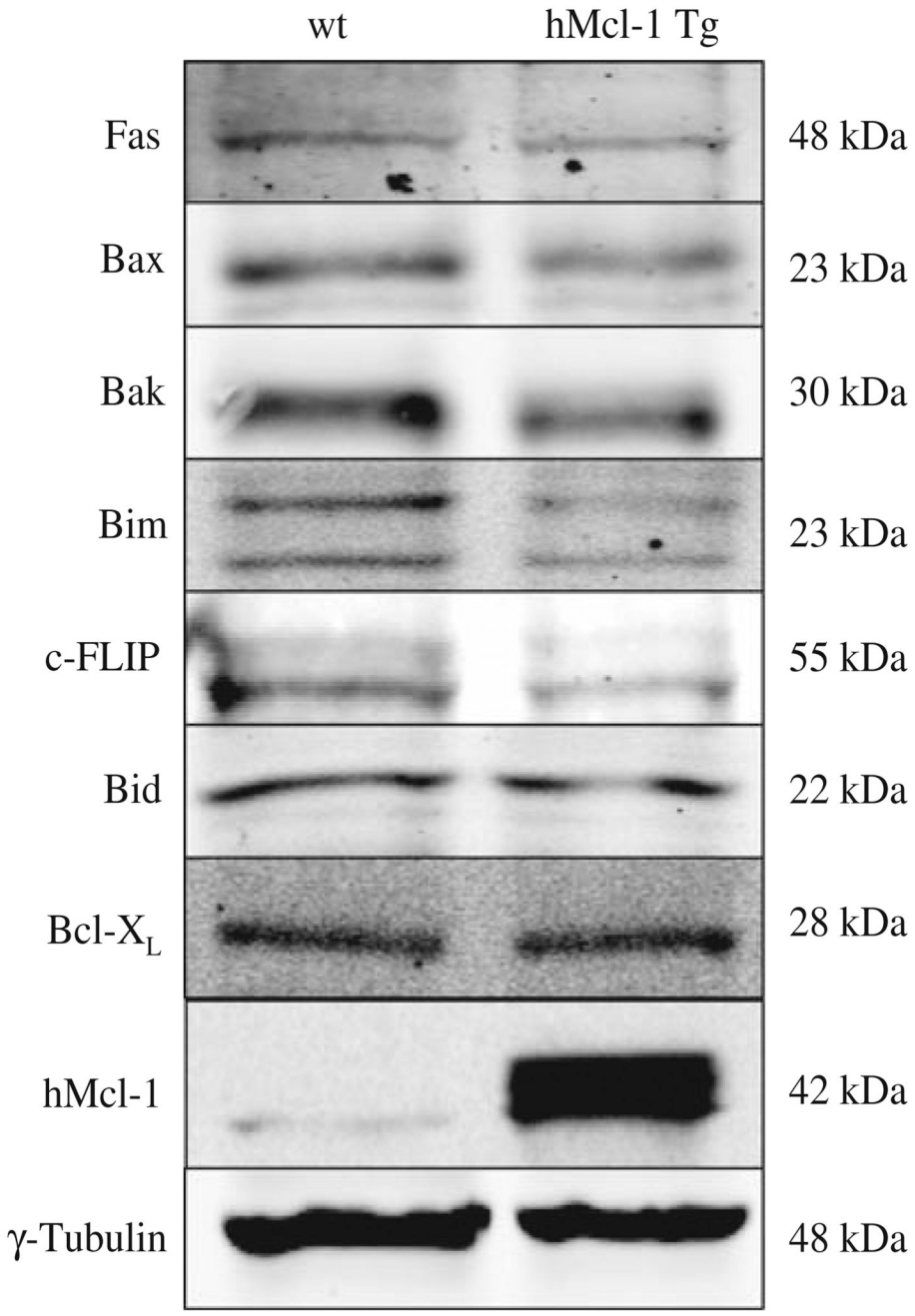

Fig. 1.

Protein expression of apoptosis effectors is similar between the different mouse genotypes under basal conditions. Aliquots of 50 μg of hepatic protein were subjected to SDS-PAGE and Western-blot analyses using antiserum to the indicated proteins. Note the expected increase in Mcl-1 signal in the hMcl-1 Tg sample. The depicted blots are representative of five separate experiments. γ-Tubulin was used as control for protein loading

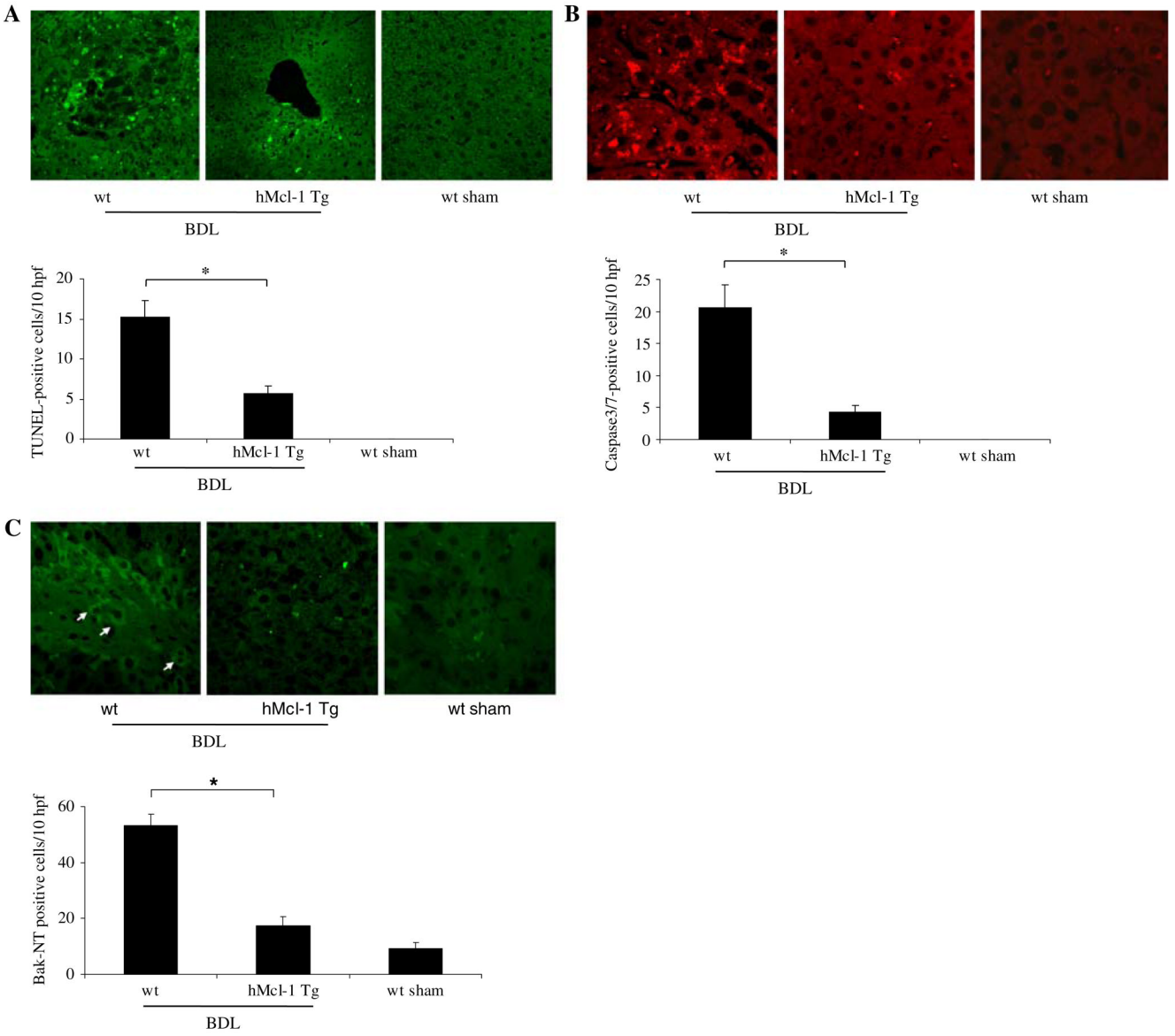

Fig. 2.

Hepatocyte apoptosis is reduced in hMcl-1 Tg mice after 7 days of BDL. **a** The number of TUNEL-positive cells was quantitated and expressed as apoptotic cells/10 high-power fields (hpf). Data are from ten independent animals per group and are expressed as the mean ± standard error. **b** Immunofluorescence for the neo-epitope of activated caspase 3/7 was performed. Cells were considered positive if staining was clearly intracellular, which is consistent with a cytoplasmic location of caspase 3/7. Occasional fluorescence in the sinusoids was not counted and appeared to reflect an artifactual signal from erythrocytes. *Data points* represent experiments from ten independent animals and *bars* are expressed as the mean ± standard error. **c** Bak N-terminal immunoreactivity was visualized by immunofluorescence and quantitated from three animals per group, mean ± standard error; $*P < 0.05$ by ANOVA for wt versus hMcl-1 Tg mice following BDL

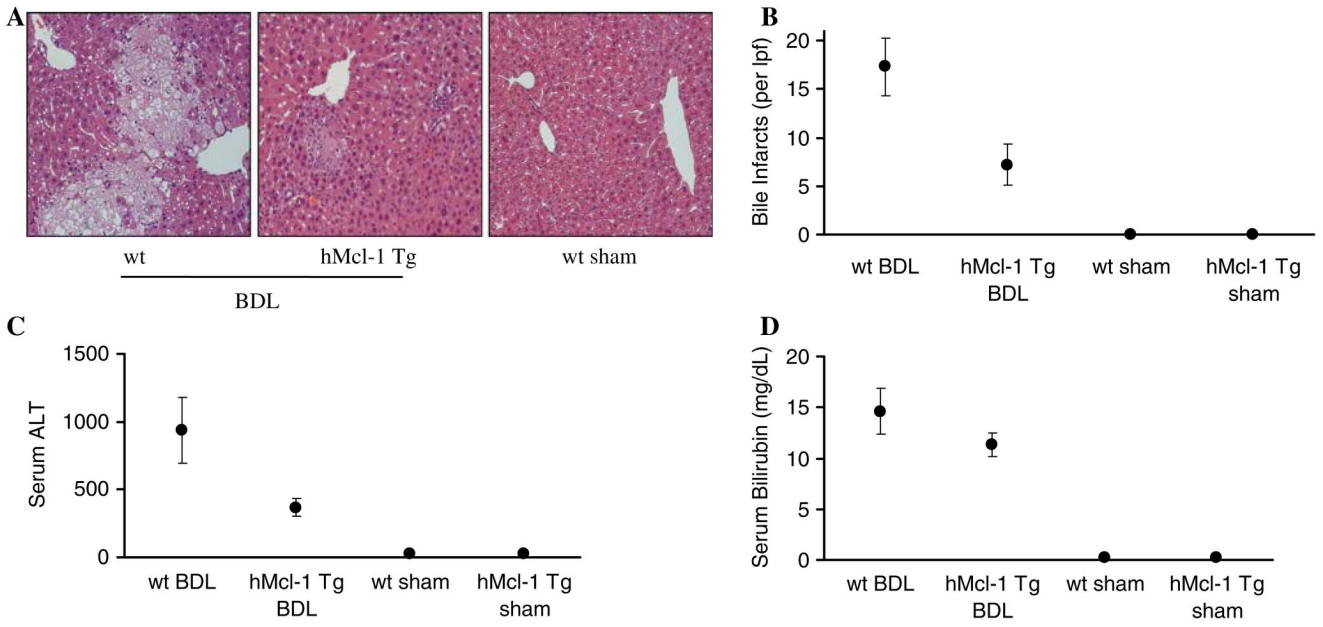

Fig. 3.

Liver injury is attenuated in hMcl-1 Tg mice after BDL. Wild-type and hMcl-1 Tg mice were subjected to common bile duct ligation. On day 7 post-surgery, mice were sacrificed to obtain liver and serum samples for histological examination and determination of liver enzymes and bilirubin levels. **a** Representative photomicrographs of conventional H&E-stained liver sections are shown (magnification 20×). Liver specimens of wild-type BDL mice displayed significant and extensive hepatocyte injury with bile infarcts, bile duct proliferation and portal edema. **b** Bile infarcts (confluent foci of hepatocyte feathery degeneration caused by bile acid cytotoxicity) were quantified in wild-type and hMcl-1 Tg mice following BDL, expressed as number per low-power field (lpf). **c** Serum ALT values were measured 7 days after BDL. **d** Serum total bilirubin determinations were quantified 7 days after BDL. Data are from ten independent animals and expressed as mean ± standard error, $*P < 0.05$ (by ANOVA) for wt versus hMcl-1 Tg mice following BDL

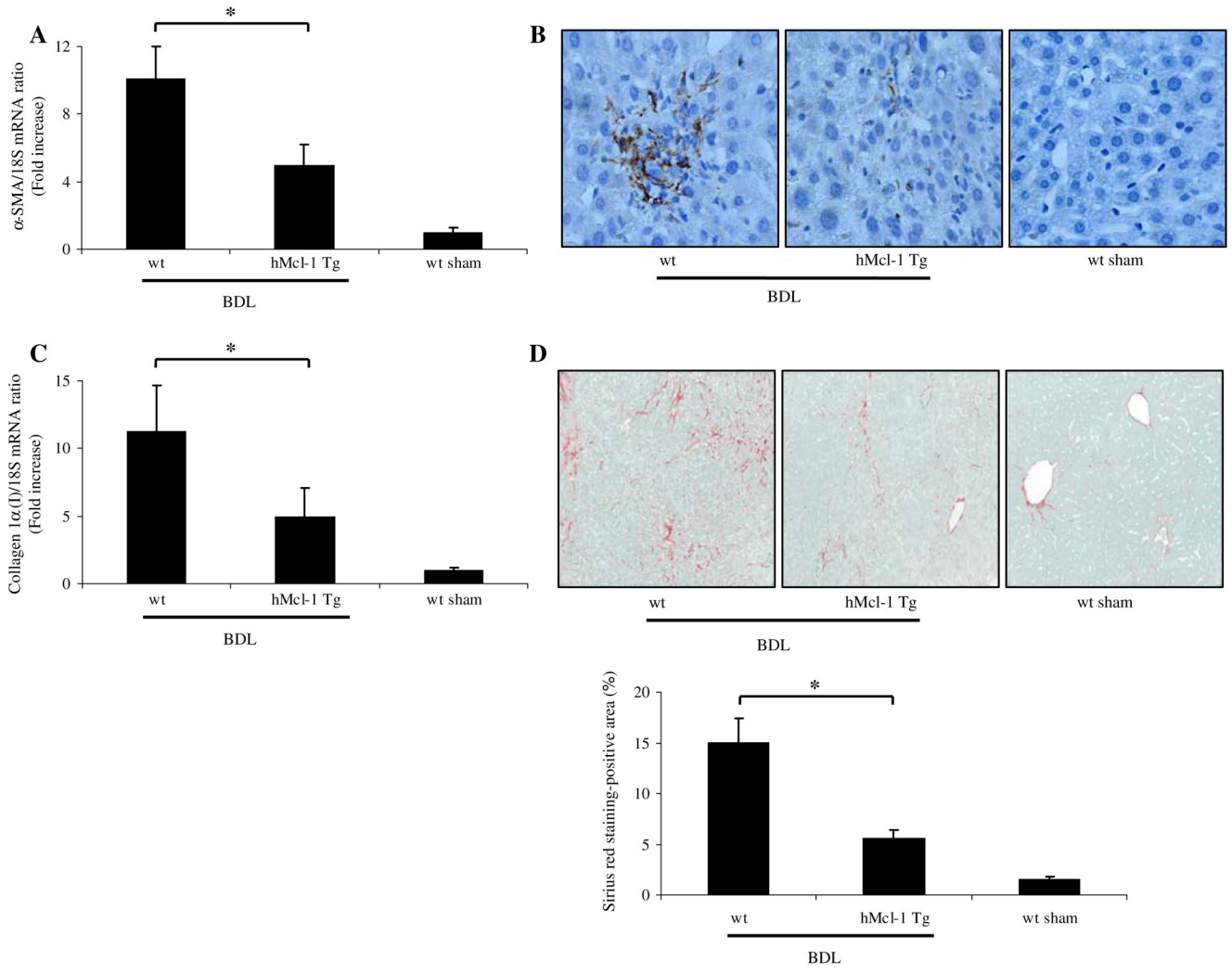

Fig. 4.

Hepatic fibrosis is reduced in hMcl-1 Tg animals 14 days post-BDL. **a** α-SMA and collagen 1α (I) mRNA expression, markers for stellate cell activation and hepatic fibrogenesis were quantified by real time-PCR. Data were obtained from ten independent animals and expressed as mean ± standard error (**P* < 0.05 by ANOVA). **b** Photomicrographs after immunohistochemistry for α-SMA following BDL of 14 days are depicted. **c** Expression of collagen 1α (I) mRNA was quantified by real time-PCR 14 days after BDL (**P* < 0.05 by ANOVA, *n* = 10 for each group). **d** Sirius red staining, a chemical stain of collagen deposition in the liver, was performed 14 days after BDL. Collagen fibers stained with Sirius red were quantitated using digital image analysis. Representative photomicrographs of liver sections from each mouse strain are depicted (magnification by light microscopy 40×; **P* < 0.05 by ANOVA, *n* = 10 for each group)

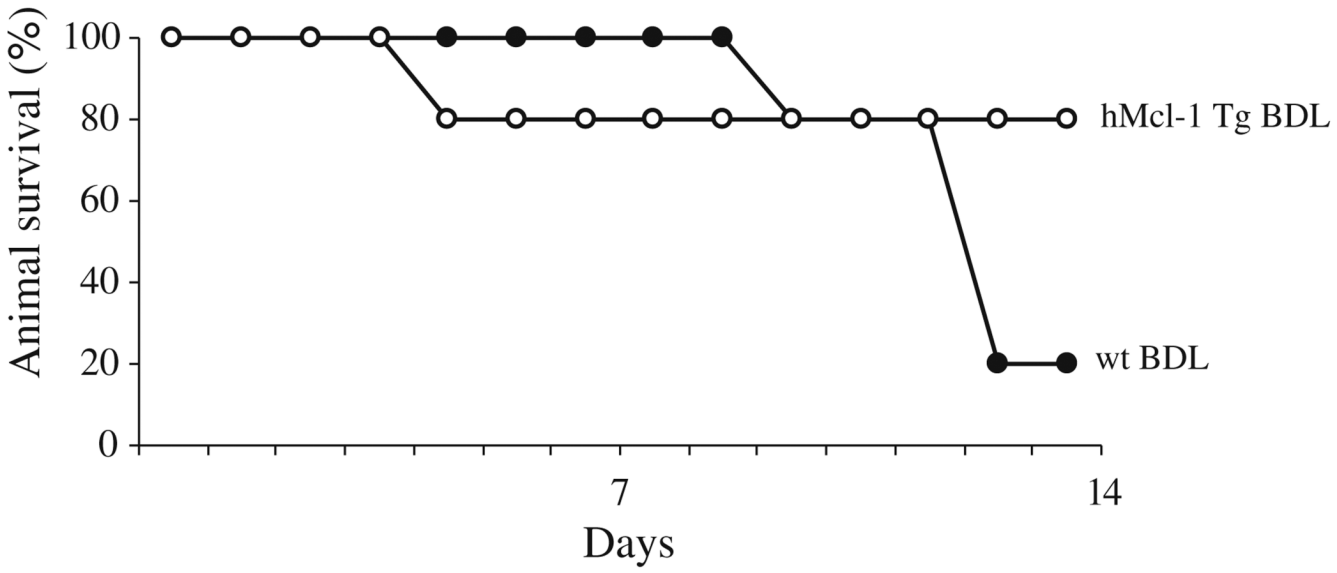

Fig. 5.
Animal survival following BDL is enhanced in hMcl-1 Tg animals. Ten animals per group were subjected to BDL and observed 14 days post-operatively